Supplementary Materials for

An improved and highly efficient geometry for facemasks

Authors: Christopher D. Cappa[1,*], The San Francisco Opera Costume Department[2,†], William D. Ristenpart,[3] Santiago Barreda,[4] Nicole M. Bouvier,[5] Anthony S. Wexler,[6] Sanziana A. Roman[7]

Affiliations:

[1] Dept. of Civil and Environmental Engineering, Univ. of California Davis; 1 Shields Ave., Davis, CA 95616 USA

[2] Costume Department, San Francisco Opera; 301 Van Ness Ave, San Francisco, CA 94102, USA

[3] Dept. of Chemical Engineering, Univ. of California Davis; 1 Shields Ave., Davis, CA 95616 USA.

[4] Dept. of Mechanical Engineering, Univ. of California Davis; 1 Shields Ave., Davis, CA 95616 USA.

[5] Dept. of Linguistics, Univ. of California Davis; 1 Shields Ave., Davis, CA 95616 USA.

[6] Department of Medicine, Division of Infectious Diseases, Icahn School of Medicine at Mount Sinai, 1 Gustave L. Levy Place, New York, NY 10029, USA

[7] Department of Surgery, Univ. of California, San Francisco; 1660 Divisadero St., San Francisco, CA 94143 USA

[†] Includes: Amy Ashton-Keller, Daniele McCartan, Galen Till, Jai Alltizer

*Corresponding author: cdcappa@ucdavis.edu or Sanziana.Roman@ucsf.edu

This PDF file includes:

Materials and Methods

Figs. S1 to S8

References

1 Materials and Methods

Mask Design

The singing mask, shown in Figure 1, uses a two-bone structure to separate the mask material from the main area of the face by about 6 cm, while still allowing for a good seal. A 0.6 cm wide, 10 cm long thin aluminum strip is used around the nose, which the wearer can mold to their face. A felt strip on the inside runs across the nose area to help with sealing. The sides of the mask extend over the cheeks, nearly to the ears. Adjustable elastic ear loops keep the sides of the mask in place and two additional ties fasten the mask around the wearer's head to further seal the mask against the face. The mask completely envelops the wearer's jaw and chin, with an adjustable elastic band below the jaw that keeps the mask tight against the neck while allowing for free jaw movement. The mask has two main regions: the upper, boned structure that holds the filtering fabric in front of but away from the mouth and nose, and an unstructured, expanded volume below the chin. The upper region is composed of three layers in a cloth-liner-cloth arrangement, with 200 thread count cloth outer layers and and Pellon® 50 inner layer attached to the cotton with a fusible webbing material. The Pellon® 50 inner layer helps to stiffen the mask material but likely provides little filtering. The length of the top region is about 12 cm. The lower expanded volume is made of two cloth layers and opens at the bottom to allow for drinking by straw during rehearsals. The opening is sealed by folding the mask twice and then securing with embedded Velcro strips. Negligible particle emissions from this area were observed after closing. When closed, the length of the expanded region is about 10 cm. A modified version of the singing mask was also constructed. The difference from the standard singing mask is that there is no bottom opening; the modified mask is otherwise identical. During use, the cloth material comprising both the singing and modified singing masks was observed to deflect inward (for inhalation) and outward (for exhalation). However, the boning provides support that limits the amount of cloth deflection associated with inhalation and exhalation. With intentionally loose wearing, the deflection magnitude decreased. Hence, deflection provides a qualitative indication of good fit. The mask internal volume is about 0.5 L. This is similar to the tidal volume associated with normal breathing (*27*), but about half that for singing (*28*). Given the limited deflection of the mask material this implies substantial exchange of air, which will help to alleviate any depletion of oxygen or buildup of CO_2.

Proper wearing of the singing masks includes: first securing the mask using the ear loops, molding the aluminum strip around the nose, tightening the ear loops, tightening the neck strap elastic band, tying the top strap around the users head near the parietal eminence, and then tying the bottom strap around the users neck while sitting or standing up straight. With proper wearing, one should see no obvious gaps, especially around the nose; this can be qualitatively assessed by having the wearer look down towards their nose moving only their eyes. If they can see their nose below the mask then there is a gap and the mask should be better secured.

Two additional masks were constructed using the same materials as the singing mask. One was constructed having only two cloth layers and one having three layers (cloth-liner-cloth). Both used a general pleated surgical mask design, based on the design initially promoted by the U. S. Centers for Disease Control; the directions and instructional video originally made available by the CDC are no longer available online. Both used the same ear loops as with the singing mask and included two head straps. Additional tests for the through-mask efficiency were performed by one participant using an N95 respirator (3M, Model 8210), two different surgical masks (a medical-grade ValuMax 5130E-SB and an unknown model), and a non-medical 'Fashion Dust Preventive Mask' (30% cotton, 70% polyester) from YiWu Xuefeng Mask Factory, both without (FDPM) and with (FDPM(N95)) an N95 insert.

Human subjects

We recruited 12 volunteers (4 self-identified male and 8 self-identified female), ranging in age from 18 to 65 years old. The Institutional Review Board of the University of California, Davis approved this work (IRB# 844369-4), and all research performed followed the Institutional Review Board guidelines and regulations. Prior to the tests, written informed consent was obtained from all participants. Information collected from participants included their age and singing range (e.g., soprano, alto, baritone). Only self-reported healthy non-smokers were included in the study. All participants had to take the UC Davis Daily Symptom Survey (https://campusready.ucdavis.edu/symptom-survey) prior to accessing campus. Participants were encouraged to obtain a negative COVID-19 test just prior to their participation, although this was not required or tracked. Informed consent for publication of identifying information was obtained from the participant shown in Figure 1.

Expiratory Aerosol Experimental Description

We used an experimental setup similar to that in previous work (*12, 13, 29*). In brief, participants were asked to breath, speak, or sing in front of a stainless steel funnel connected by nonconductive tubing to both an aerodynamic particle sizer (APS, TSI Model 3321, 5 L/min) and a condensation particle counter (CPC, TSI Model 3775, 0.3 lpm) that were located in a HEPA-filtered laminar flow hood. The APS characterizes particles from 0.3 to 20 microns in aerodynamic diameter, with a decreased detection efficiency for particles <0.5 microns and the smallest size reported as 0.5 microns. The CPC characterizes the number concentration of all particles sampled, although with a reduced efficiency for particles larger than about 1 micron owing to impaction losses.

Participants donned the singing mask without direct assistance. They were asked to tighten the ear loops and the neck closure, pinch closed the metal bar in the singing mask around their nose, and to tie the neck and head straps. They were asked to "tighten everything as much as possible, but such that you are still comfortable."

Respiratory emissions with or without a mask were tested with the participant's head oriented in one of four positions, relative to the sampling funnel. These orientations were the same as those described in Cappa et al. (*14*) and are shown in Figure S3. These were as follows.

(i) *Forward/Through*: The participants sat directly facing the APS funnel. This was the orientation examined in prior studies (*12, 13, 29*). In this orientation, the APS samples air that has passed through the mask material.

(ii) *Top*: The participants tilted their heads downward to have the bridge of the nose approximately centered on the APS funnel, allowing for sampling of particles that leak from the mask nose area.

(iii) *Side*: The participants turned their head 90 degrees to face perpendicular to the APS funnel, with the side singing mask approximately centered on the funnel

(iv) *Bottom*: The participants positioned their chin just above the APS funnel with the mask material from the expanded volume over the top of the funnel. This allowed for sampling of particles that leak from the mask neck area.

Participants performed the speaking and singing activities while either wearing or not wearing the singing singing mask. Breathing was performed only with no mask. For speaking, participants were asked to read the "Rainbow Passage," both with no mask and while wearing the mask while oriented in the "forward" direction (Figure S3). Participants also performed two singing activities. First, they sang in English Beethoven's *Ode to Joy* from his Ninth Symphony, both wearing and not wearing the mask in each of four head orientations described above (Figure S3). Second, participants sang a song of their choosing of about two minutes in length. They performed this second activity both without a mask and with the mask in the forward orientation only.

For all speaking and singing activities, participants were asked to carry out the activity at a comfortable volume; no effort was made to control for volume differences between participants. While loudness can influence the emission rate of expiratory aerosols (*12*), we focus on the reduction achieved by wearing the mask, and thus loudness differences will have little effect. All particle emission rates were adjusted to units of particles per second by accounting for the actual duration of vocalization (t_{voc}), which excludes pauses between words or phrases as determined from microphone recordings. One participant repeated the *Ode to Joy* activities multiple times on different days.

The directly observed particle emission rates ($\dot{N}_p^{obs}$) does not necessarily equate to the total particle emission rate owing to differences between the APS total airflow rate (5 lpm) and the airflow rate of the expiratory activity ($Q_{exp,tot}$), as discussed in Cappa et al. (*Submitted*).(*14*) This raises certain challenges when combining the measurements from the different orientations to estimate the overall mask efficiency. Typical airflow rates associated with talking range from ca. 8-15 lpm (*30*). For singing, airflow rates are in the same general range although skewed perhaps a little higher, especially for louder singing, and females tend to exhibit slightly smaller values than males (*31, 32*). Consequently, the actual particle emission rates associated with talking and singing without a mask are about a factor of 8-15 times higher than the observed values. We present the unadjusted (observed) absolute values to remain consistent with previous studies.

With mask wearing the airflow during expiration can be split in multiple directions, with the amount of air in a given direction not known *a priori*. We previously accounted for this split for surgical masks while talking or coughing using a Monte Carlo method to determine probability distributions of the overall mask efficiency based on the median values across the population of

participants (*14*). Overall, relatively narrow probability distributions resulted with only moderate sensitivity to the assumed split between the air that passed through the mask versus escaped out the top, sides, or bottom and the greatest deviations found for very low total expiratory airflow rates. We used a similar approach here, but applied the approach to the observations from each individual, rather than using the medians across participants. Over 10,000 iterations, we determined the fraction (f_x) of air that goes in a particular direction from a random distribution. We further assumed a log-normal distribution of expiratory airflow rates centered at 13 lpm with a width of 1.3. The $\dot{N}_{p,i}^{obs}$ in each orientation (i) for each individual are adjusted to actual particle emission rates ($\dot{N}_{p,i}$) based on the above assumptions. While we present the unadjusted (observed) absolute values to remain consistent with previous studies, when reporting particle emission rates normalized to the no-mask condition we use the airflow-adjusted values, which are also used to calculate the overall mask efficiency. The overall mask efficiency, η, is:

$$\eta = 1 - \frac{\sum \dot{N}_{p,i}}{\dot{N}_{p,nomask}}$$

The average value and standard deviation for each individual were determined from the distribution of η values from the simulations.

In the "bottom" orientation, the participants positioned their chin just above the APS funnel, with the mask material from the expanded volume draped over the top of the funnel. Some participants could not completely avoid contact between the mask material and the funnel in this position; consequently, mask fibers shed by friction between mask and funnel may have contributed to the particle counts from participants in this orientation.(*13, 33, 34*) Such non-expiratory particles confound the respiratory emission measurements, but they may still carry pathogens as aerosolized fomites (*35*). Based on the observed particle size distributions, a few participants appeared to generate a significant amount of mask-fiber particles. For these participants, when assessing the overall mask efficiency, we used the median value from the other participants in place of the value measured for the individual.

One participant sang *Ode to Joy* wearing a variety of mask types (see *Mask Design*) in the forward (through-mask) position, with three replicates for each mask type.

All data processing analyses were carried out using Igor Pro (v. 8.0.4.2, Wavemetrics). Differences between the $\dot{N}_{p,i}$ values are calculated after log-transformation using a single factor ANOVA test.

Inhalation Experimental Description

The concentration of particles inside the singing mask was measured for one participant while breathing. Here, a tube composed of conductive silicon was inserted below the mask at the neck area and the sampling end of the tube was positioned to sit in the main mask area in front of the face. The tube was attached to a condensation particle counter, which sampled at 0.3 lpm and measured the total concentration of particles every 1 second. Two experiments were conducted. In both, the participant was asked to breathe deeply in and out through their nose 10 times at a rate of about five breaths per minute while the particle concentration inside the mask was continually monitored. In one experiment, the neck strap was fully tightened, as appropriate for correct fit of the singing mask. For the second, the neck strap was left slightly loose to intentionally introduce a leak. Prior to starting the measurement, the participant was asked to breathe three times after the sampling tube was inserted. The concentration of particles in the room air was measured just prior to the measurements of particle concentrations inside the mask.

Filtration Efficiency versus Distance Experimental Description

The influence of the mask-face separation distance on filter efficiency was characterized as follows. A fibrous filter having moderate efficiency was secured over the APS sampling funnel using an elastic band. This provided the filtration material, and the "mask"-face separation distance was characterized as the distance between the participants' mouth and the fibrous filter. To eliminate the influence of the air from the laminar flow hood on the measurements, a cylindrical sheath having the same diameter as the APS sampling funnel was constructed out of aluminum foil. The sheath was secured to the APS sampling funnel using a second elastic band to make a seal. The distance that the sheath extended from the APS sampling funnel could be adjusted over the range 1 cm to 10 cm. A schematic is shown in **Error! Reference source not found.**. Background concentrations were unaffected by the presence of the sheath. Without this sheath, the measured particle concentrations during speaking the *Rainbow Passage*, and without the fibrous filter, would decrease as the participant moved further from the APS sampling funnel. More specifically, without the sheath the measured concentration was constant within measurement

reproducibility when the participant was within 3 cm of the plane of APS sampling funnel but decreased with further distance. With the sheath (and without the filter), there was no discernible change in the measured concentration with distance.

A participant was asked to recite the *Rainbow Passage* with the sheath set at distances ranging from 1 to 10 cm. The participant gently placed the bridge of their nose and their chin against the sheath to maintain a given distance throughout the activity. Because the participant's mouth extended ~0.5 cm into the sheath, the reported distances are 0.5 cm less than the length of the sheath. The participants face did not entirely cover the sheath. Because the sheath was sealed to the sampling funnel, excess air from speaking (relative to the APS flow) exited by the participants face. The distances were selected in a random order. At each distance three replicates were performed with the fibrous filter in place over the APS sampling funnel and compared to the measurements made with no filter.

The particular fibrous filter used necessarily exhibited little fiber shedding and also had a moderate overall filtration efficiency. The latter condition is necessary because if the filtration efficiency is too large it is difficult to determine changes with distance quantitatively within the measurement uncertainty, and working with a fibrous filter having a moderate (~50%) efficiency allows for access of a greater range of values. To meet these requirements, we used the outer layer of a 3-layer surgical mask as the fibrous filter, specifically the outer layer of the ValuMax 5130E-SB mask. (The inner layer of this mask had too high of an efficiency. The singing mask, despite limited evidence of substantial shedding when worn by the participants, shed particles excessively when secured over the APS sampling funnel.)

The total filtration efficiency was determined by summing over all particles measured. The size-dependent filtration efficiency was determined in 5 size bins: the lower size limit to 0.8 μm, 0.8-1.25 μm, 1.25-1.9 μm, 1.9-3.9 μm, and 3.9-10 μm. Uncertainties were taken as the 1σ standard deviation of the mean over the three replicates.

Influence of face-mask separation distance on filtration efficiency

For an expiratory jet, the air velocity, u, decreases with distance as $1/(\alpha \cdot x)$, where α is the divergence angle (~20°) and x is distance (*20*). Overall filtration efficiencies (η_f) for fibrous filters vary as:

$$\eta_f = 1 - \exp(-K \cdot \eta_{SF}) \quad \text{(S1)}$$

where η_{SF} is the single-fiber filtration efficiency accounting for losses by diffusion, interception, and impaction and *K* is a constant dependent on the filter packing density, thickness, and fiber size (*19*). For diffusion-driven losses,

$$\eta_{SF,diff} \propto Pe^{-\frac{2}{3}} \propto u^{-\frac{2}{3}}, \quad \text{(S2)}$$

and where *Pe* is the Peclet number, which is proportional to velocity (*u*) through the filter (*19*). Loss via interception and impaction has a more complex relationship with conditions, but can be approximated as

$$\eta_{SF,int+imp} \sim 10\text{^}\left[y_0 + \frac{abs(y_0)}{1+\exp\left(\frac{(\log(Stk_0)-\log(Stk))}{r}\right)}\right], \quad \text{(S3)}$$

where *Stk* is the Stokes number, which is proportional to velocity and the other terms are constants that depend on the fiber size and the particle diameter (*19*). The overall single-fiber efficiency is then:

$$\eta_{SF} = \eta_{SF,diff} + \eta_{SF,int+imp} - \eta_{SF,diff} \cdot \eta_{SF,int+imp}. \quad \text{(S4)}$$

Rewriting Eqn. S2 and S3 to depend on the mask-face separation distance, *x*, rather than velocity, we have:

$$\eta_{SF,diff} = A \cdot x^{\frac{2}{3}}, \quad \text{(S5)}$$

and

$$\eta_{SF,int+imp} \sim 10\text{^}\left[y_0 + \frac{abs(y_0)}{1+\exp\left(\frac{(-\log(x_0)-\log(x))}{r}\right)}\right]. \quad \text{(S6)}$$

Substitution of Eqn. S5 and S6 into Eqn. S4, and the resulting expression into Eqn. S1 yields an expression for the overall filtration efficiency that depends on the mask-face separation distance, and which can be fit to observations.

2 Supplemental References

1. S. Hallett, F. Toro, J. V. Ashurst, Physiology, Tidal Volume, in *StatPearls [Internet]* (StatPearls Publishing, Treasure Island, FL, 2020), Accessed on: 2 February 2021, https://www.ncbi.nlm.nih.gov/books/NBK482502/.
2. B. Binazzi *et al.*, Breathing pattern and kinematics in normal subjects during speech, singing and loud whispering. *Acta Physiologica* **186**, 233-246 (2006).
3. S. Asadi *et al.*, Effect of voicing and articulation manner on aerosol particle emission during human speech. *PLoS One* **15**, e0227699 (2020).
4. J. K. Gupta, C.-H. Lin, Q. Chen, Characterizing exhaled airflow from breathing and talking. *Indoor Air* **20**, 31-39 (2010).
5. J. J. Jiang, R. B. Hanna, M. V. Willey, A. Rieves, The Measurement of Airflow Using Singing Helmet That Allows Free Movement of the Jaw. *Journal of Voice* **30**, 641-648 (2016).
6. E. B. Holmberg, R. E. Hillman, J. S. Perkell, Glottal airflow and transglottal air pressure measurements for male and female speakers in soft, normal, and loud voice. *The Journal of the Acoustical Society of America* **84**, 511-529 (1988).
7. D. Hospodsky *et al.*, Human Occupancy as a Source of Indoor Airborne Bacteria. *PLoS One* **7**, e34867 (2012).
8. R. P. Clark, S. G. Shirley, Identification of Skin in Airborne Particulate Matter. *Nature* **246**, 39-40 (1973).
9. S. Asadi *et al.*, Influenza A virus is transmissible via aerosolized fomites. *Nature Communications* **11**, 4062 (2020).

3 Figures

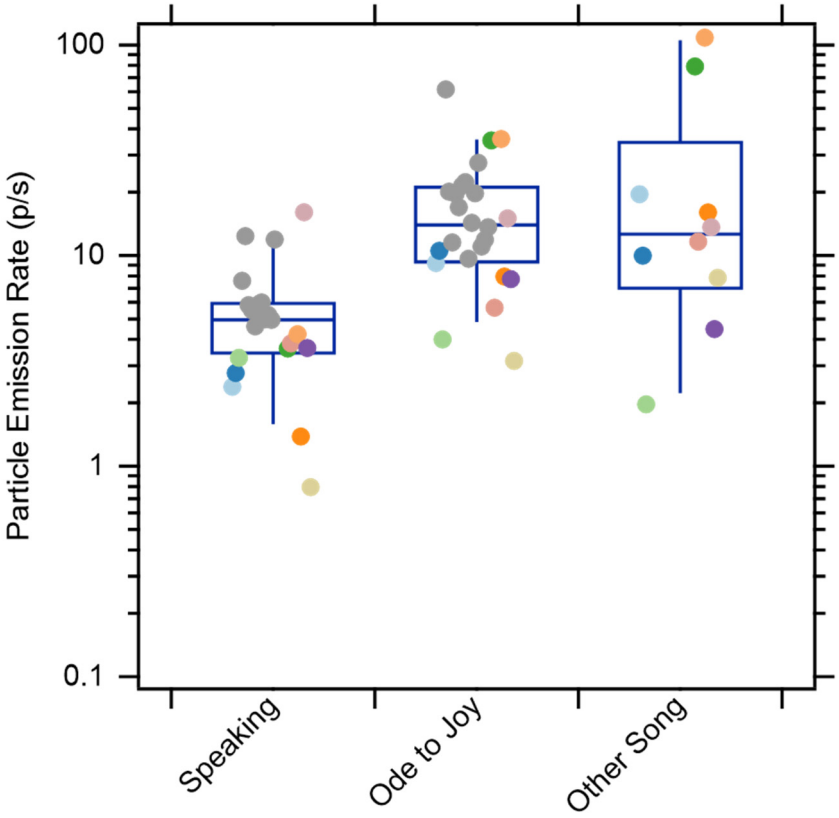

Figure S1. Observed particle emission rates (p/s) for the individual participants without mask wearing. These have not been corrected for undersampling by the APS (see methods). Emissions from the singing activities are three times greater than for speaking; the difference is statistically significant ($p = 0.002$). Points are colored by participant, with the gray dots indicating repeats from one individual.

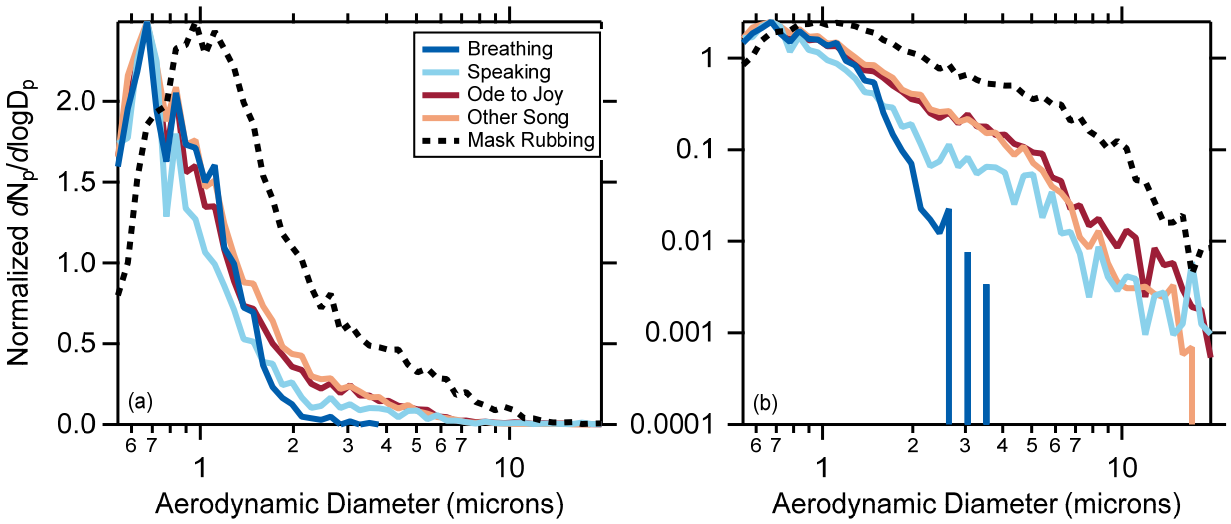

Figure S2. Particle emission rate size distributions for various expiratory activities (solid lines), i.e., breathing, speaking, and singing either the *Ode to Joy* or a song of the participants choice, and the size distribution resulting from physical rubbing of the mask material against itself (dashed line). All distributions are averages across the participants. The distributions are shown on (a) linear or (b) logarithmic y-axes.

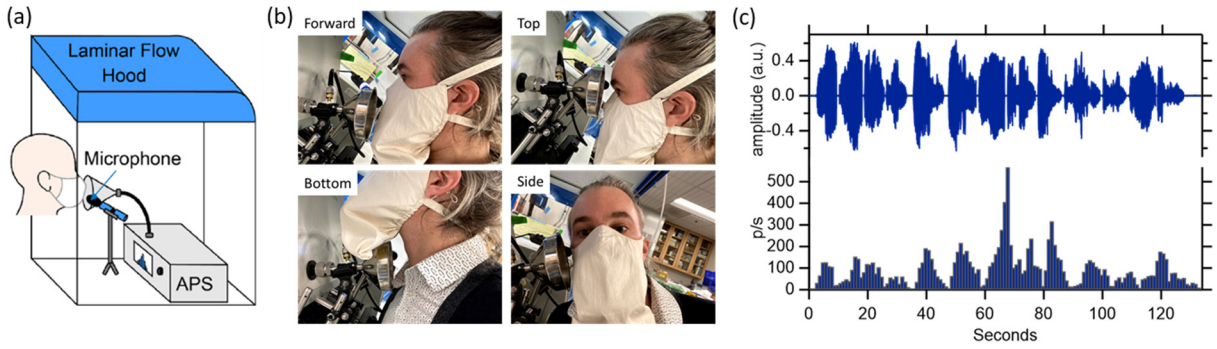

Figure S3. (a) Schematic of the experimental setup showing a participant wearing a mask in the forward orientation. (b) Photographs showing a participant in each of the four sampling orientations: forward, top, side, and bottom sampling. (c) Example microphone recording for a participant singing a song of the participants' choice without a mask and the associated particle counts by the APS.

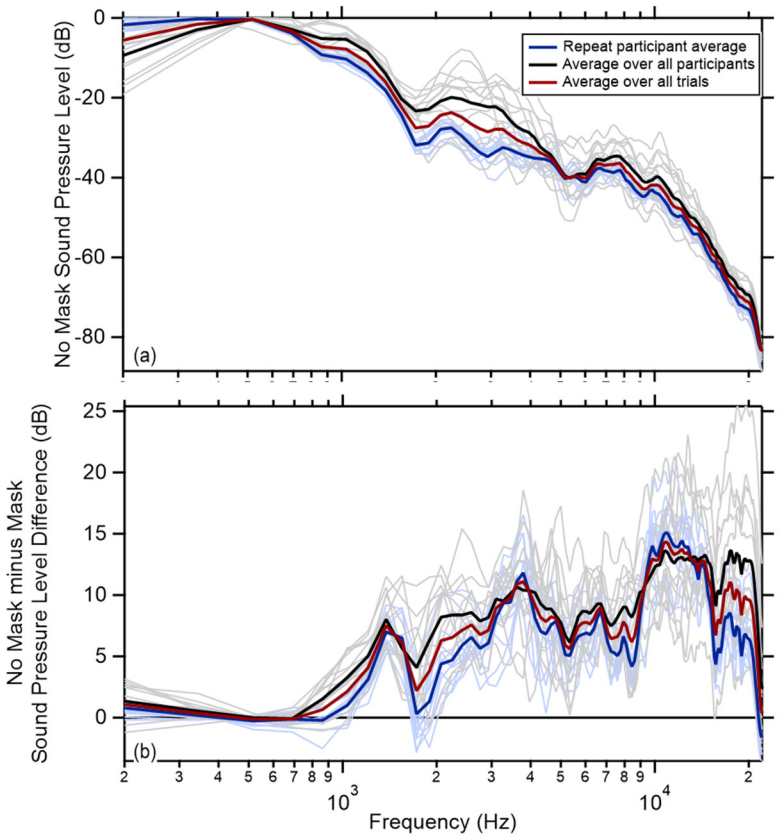

Figure S4. (a) Average power spectrum with no mask, set to full scale, and (b) difference between no mask and mask for participants singing *Ode to Joy*. Thin lines are individual measurements, with blue lines for the participant who performed replicate trials. The solid lines are averages across participants for (red) all individual trials, (blue) the repeat performer, and (black) over all participants using the average from the repeat performer.

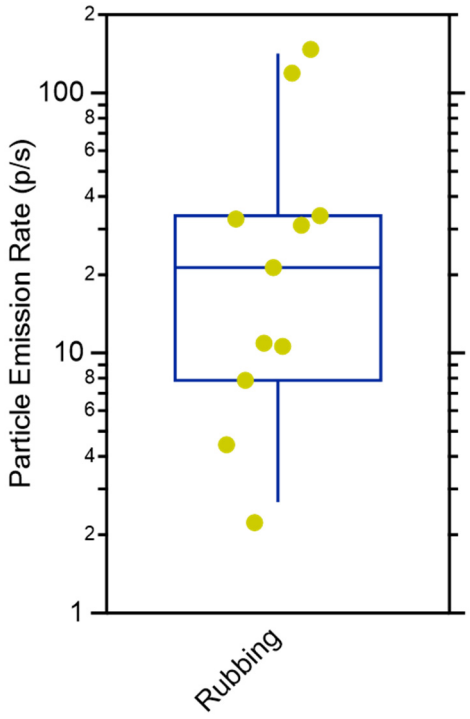

Figure S5. Observed particle emission rates (p/s) for rubbing the singing mask material together.

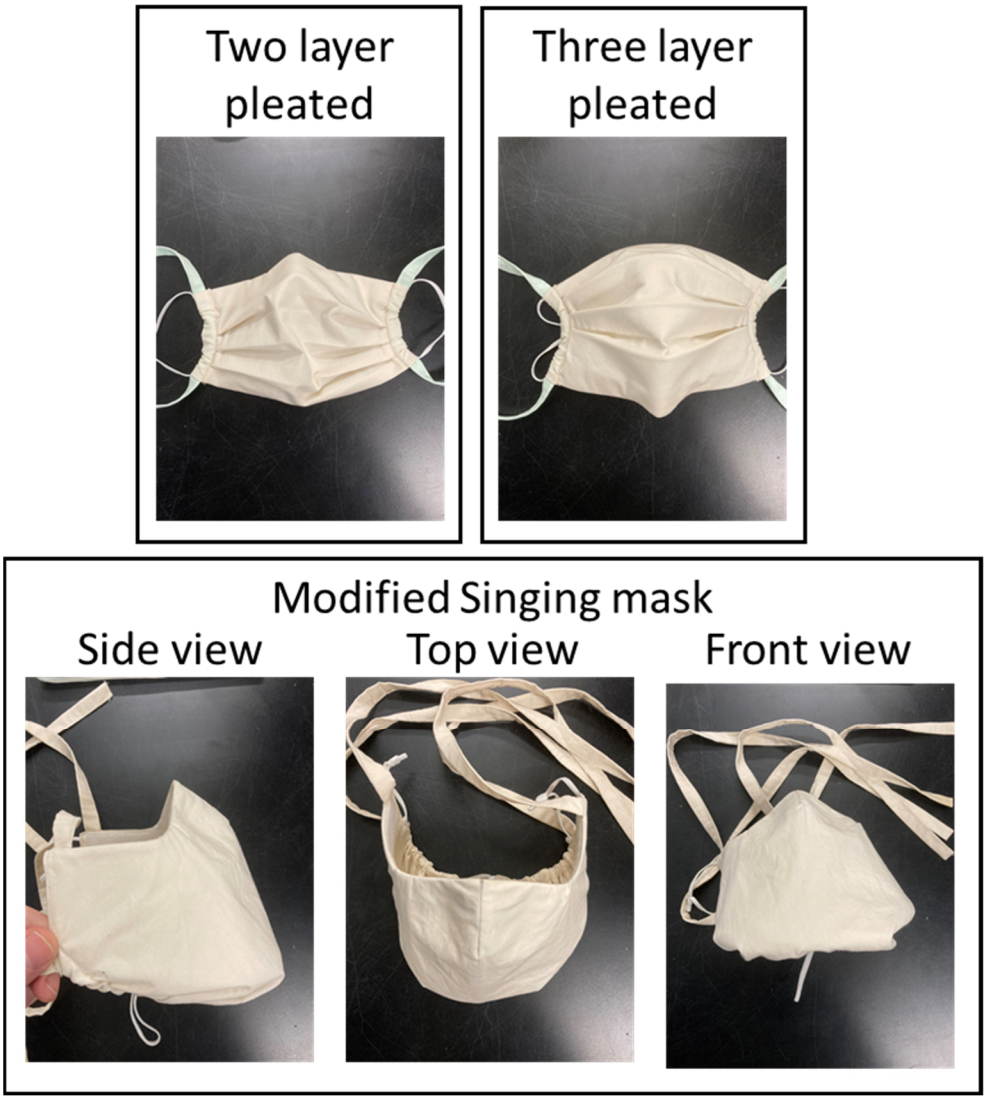

Figure S6. Photographs of the two-layer and three-layer pleated masks and the modified singing mask.

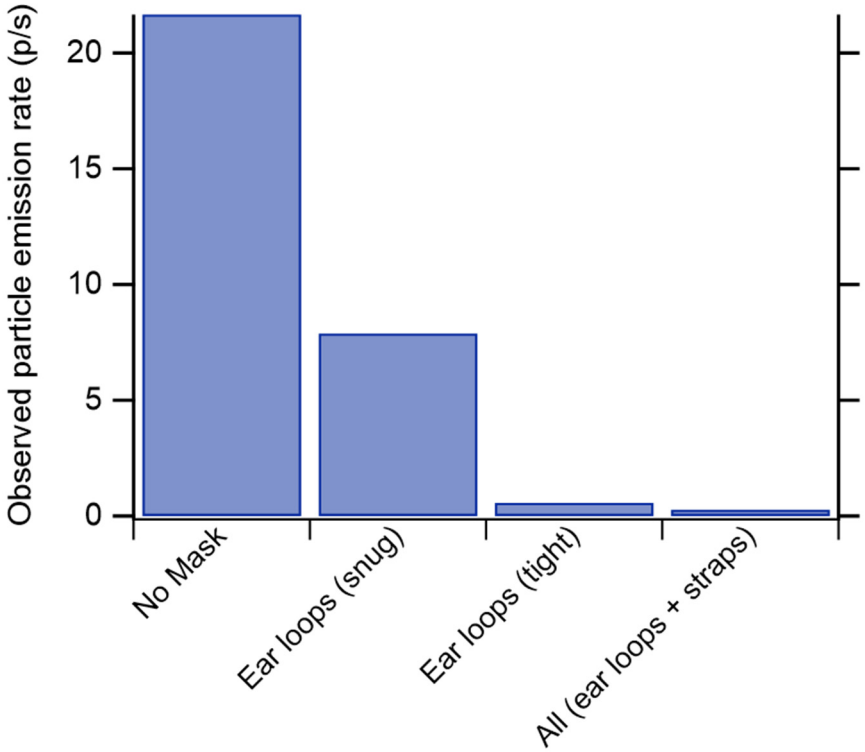

Figure S7. Observed particle emission rates (p/s) without a mask or for sampling from the top quadrant with the singing mask worn with snug ear loops only, tight ear loops-only, or tight ear loops plus the head straps.

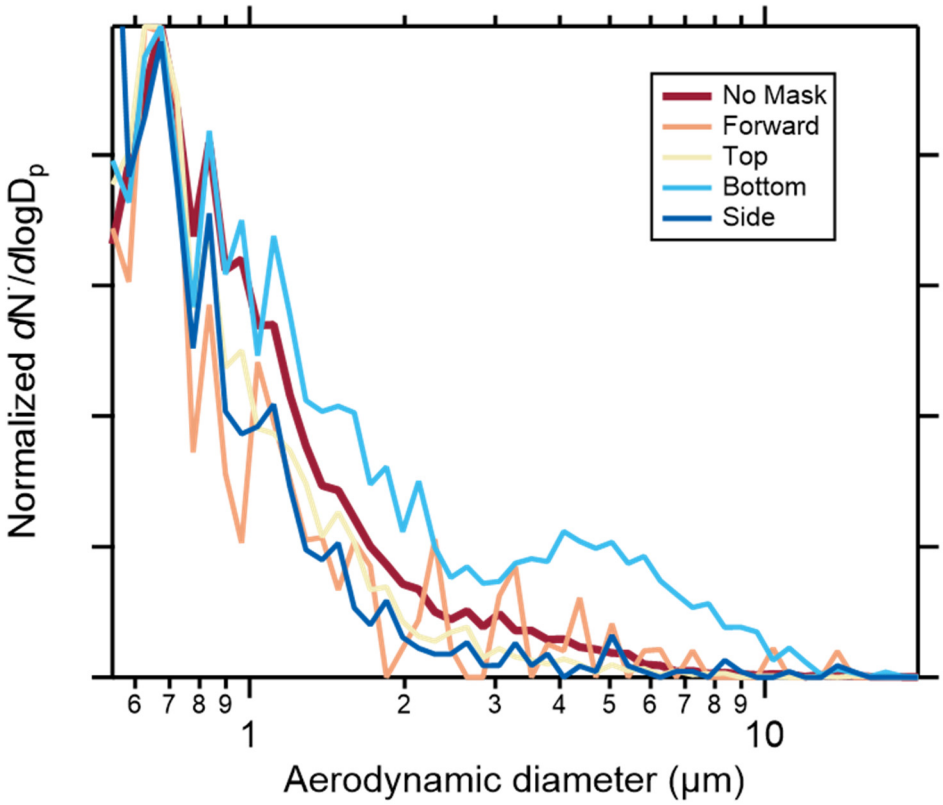

Figure S8. Normalized average particle emission rate size distributions for sampling with no mask or with the singing mask from different quadrants. Note the enhanced contribution of large particles (3-9 microns) when sampling from the bottom quadrant, indicative of fiber shedding.